

Journal of Climate

Interactions between hydrological sensitivity, radiative cooling, stability and low-level cloud amount feedback.

--Manuscript Draft--

Manuscript Number:	JCLI-D-16-0895
Full Title:	Interactions between hydrological sensitivity, radiative cooling, stability and low-level cloud amount feedback.
Article Type:	Article
Corresponding Author:	Mark Webb Met Office Exeter, UNITED KINGDOM
Corresponding Author's Institution:	Met Office
First Author:	Mark Webb
Order of Authors:	Mark Webb Adrian Lock Hugo Lambert
Abstract:	<p>Low-level cloud feedbacks vary in magnitude, but are positive in most climate models, due to reductions in low-level cloud fraction. This study explores the impact of surface evaporation on low-level cloud fraction feedback by performing climate change experiments with the aquaplanet configuration of the HadGEM2-A climate model, forcing surface evaporation to increase at different rates in two ways. Forcing the evaporation diagnosed in the surface scheme to increase at 7%/K with warming (more than doubling the hydrological sensitivity) results in an increase in global mean low-level cloud fraction and a negative global cloud feedback, reversing the signs of these responses compared to the standard experiments. The Estimated Inversion Strength (EIS) increases more rapidly in these surface evaporation forced experiments, which is attributed to additional latent heat release and enhanced warming of the free troposphere. Stimulating a 7%/K increase in surface evaporation via enhanced atmospheric radiative cooling however results in a weaker EIS increase compared to the standard experiments and a slightly stronger low-level cloud reduction. The low-level cloud fraction response is predicted better by EIS than surface evaporation across all experiments. This suggests that surface-forced increases in evaporation increase low-level cloud fraction mainly by increasing EIS. Additionally our results show that increases in surface evaporation can have a very substantial impact on the rate of increase in radiative cooling with warming, by modifying the temperature and humidity structure of the atmosphere. This has implications for understanding the factors controlling hydrological sensitivity.</p>



Click here to access/download

Cost Estimation and Agreement Worksheet
JClimate_Cost_Estimation_and_Agreement_Worksheet.
pdf

Response to Editor and Reviewer comments on "Interactions between hydrological sensitivity, radiative cooling, stability and low-level cloud amount feedback." by Mark Webb, Adrian Lock and Hugo Lambert.

We are grateful to the reviewer and the editor for their helpful comments which have helped us to improve the paper.

Responses to comments from the Editor:

L. 244 *Figure 1(f)*

Done. Manuscript amended (L244)

L. 464. *Indicate radiative cooling rate corresponds to squares. Or put a legend of symbols on Fig. 4(d).*

We now indicate that the radiative cooling rate corresponds to squares. Manuscript amended (L464)

L. 471-475. *The description doesn't match the text in boxes in Fig. 5. For example, "enhanced free tropospheric warming" is not in the diagram. How about: "... and is summarised in Figure 5 (blue arrows). As shown above, enhanced evaporation at the surface leads to enhanced free tropospheric warming (reduced lapse rate)." You could then delete "via an enhanced free tropospheric lapse rate feedback." And I think "in part due to enhanced emission of outgoing longwave radiation to space" is probably not necessary as well.*

Done. Manuscript amended (L471-474)

L. 505. *Indicate colors for experiments.*

Done. Manuscript amended (L503-507)

L. 526. *"_to_ maintain the _same_ near-surface ..."*

Done. Manuscript amended (L527)

L. 557. *Maybe indicate orange and grey lines in text?*

Done. Manuscript amended (L558-559)

L. 558-559. *Enhanced warming compared to what?*

We now write "This in turn can explain the enhanced warming in the upper troposphere in APEC4KSurfaceEvap0% (orange) compared to APEC (grey) in Figure 2(c))."

Manuscript amended (L560-561)

L. 571. *This sounds like the sign reverses as you go from APEC4K to APECSurfEvap7%. But I think the sign reverses compared with the 0% experiment?*

We now write "**With** the surface evaporation increases in the APEC4K, APECSurfaceEvap3% and APECSurfaceEvap7% experiments, the sign of the response of the air-sea temperature difference reverses **compared to that in APEC4KSurfaceEvap0%**, with the near-surface air temperature warming more than the surface, and the magnitude of the **(negative)** air-sea temperature difference reducing (Figure 4(g))."

Manuscript amended (L571-574)

L. 581. *"APEC4KRadCool7%_compared to_ APEC4K"*

Done. Manuscript amended (L583)

L. 587. *Rather than the "responses of sensible heat flux", maybe the "decreases", so it's clear that increases in wind speeds cannot cause the decreases?*

We now write "**The decreases** of the sensible heat fluxes **in response** to increases in surface evaporation and radiative cooling..." Manuscript amended (L589)

L. 606. *It might be useful to include the bulk formula here*

We prefer to point the reader to Eq 1 of Richter and Xie (2008). Manuscript amended (L608)

L. 609. *Mean monthly values are averaged to get annual average in Table 2?*

We now write "Long term averages of these predicted monthly values..." Manuscript amended (L612)

L. 616: *"muted increase" compared to what? What's expected from an SST-only change?*

We now write "These calculations show that the muted evaporation increase in the standard APEC4K experiment (**weaker than the 7 %/K increase which would occur with surface warming in the absence of changes in near-surface relative humidity, wind speed and air sea temperature difference**) is primarily due to increases..."

Manuscript amended (L617-619)

L. 619. *A "comparable" contribution seems a little contradictory to the "primary" effect of enhanced winds.*

Modified to say "secondary". Manuscript amended (L623)

L. 626. *What are "these quantities"?*

We now write “These results also demonstrate however that the responses in **the factors controlling the surface evaporation (such as near-surface relative humidity, wind speed and air-sea temperature differences)** are affected...”

Manuscript amended (Text now at L710-711 - see below)

L. 667. Implies that in some cases EIS does change substantially in the radiative experiment. Add a comma between "experiment" and "in"?

Done. Also added missing “in” to read “Substantial low cloud reductions are also seen **in** the radiative cooling forced experiment, in the absence of substantial changes in EIS.”
Manuscript amended (L670)

L. 707. "artificially enhancing the radiative cooling with warming" sounds a little contradictory. "artificially enhancing the radiative cooling by warming the atmosphere"?

We now write “Meanwhile, artificially enhancing the radiative cooling **increase which accompanies surface warming...**”
Done. Manuscript amended (L700)

L. 714. This paragraph is almost the same as that at the end of the previous section. Unlike the reviewer, I actually prefer this paragraph here, but agree that it is repetitive, and it would be nice to shorten one of the two.

Agreed. We have removed the paragraph at the end section 3 and merged it in to the paragraph at the end of the conclusions. This now reads:

“It is widely appreciated that increases in near-surface relative humidity will act to damp increases in surface evaporation, while increases in the magnitude of air-sea temperature differences and near-surface wind speeds will act to enhance it. Our results also demonstrate however that the responses in **the factors controlling the surface evaporation (such as near-surface relative humidity, wind speed and air-sea temperature differences)** are affected not only by radiative cooling but also by changes in surface evaporation itself. **We argue that the** hydrological sensitivity will **ultimately** be determined by the point at which various interacting responses in **near-surface relative humidity and wind speed, air-sea temperature difference, surface evaporation, sensible heat fluxes and radiative cooling** come into a new balance **following a given surface warming**. This means that a full understanding of the mechanisms controlling hydrological sensitivity differences in models will require a better appreciation of these various inter-dependent responses. These insights may help to improve our understanding of the factors controlling hydrological sensitivity in the future.”

Manuscript amended (L710-715)

Reviewer #3:

Overall, I have very little to say. The authors have adequately addressed my previous comments. I appreciate their efforts, and I think the revised manuscript is more clear and impactful for the changes. The addition of Figure 3 is especially helpful in linking the results to the model physics. The goal of the paper is clear, the methodology is appropriate, the analysis is well done, and the conclusions are supported. This paper fits well in the current literature, and will help to inspire additional studies.

My only remaining criticism is that the paper is still a little long. The discussion of the new panels of Figure 4 and the regression analysis of Table 2 seem like they could be tightened up.

We have made various minor edits to shorten the sections of text mentioned. Please refer to the tracked changes version to see these.

Manuscript amended (L495-625 in the main manuscript, 516-623 in the tracked-change version)

The "Summary and Conclusions" section could also be shortened substantially. I noted that some of the text in that section is nearly identical to previous sections. For example, the last paragraph (l 714-722) is basically the same as the last paragraph from the preceding section (l 623-632). The repetition is not inherently bad, but I think that the summary should be more concise, just giving the essence of the results.

We have dealt with the duplicated text by removing it from the results section and merging in with the conclusions (see above comment from the editor.) We have also made various minor edits to shorten conclusions section. Please refer to the tracked changes version to see these.

Manuscript amended (L646-698 in the main manuscript, L664-716 in the tracked-change version)

As for the conclusions just giving the essence of the results, I know that there are different views on this. There are so many papers to read these days that many people just read the conclusions and skim the rest. Personally I prefer a more comprehensive summary, and this policy has served me well in the past.

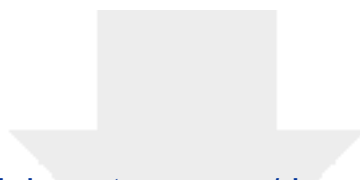
Additional changes.

We corrected an error in the units on Figure 2(a,b) (changing K/K to K).

On re-reading we thought it clearer to add "in a uniform +4K SST perturbation experiment" to line 633-634.

We also added "We are also grateful to Karen Shell and two anonymous reviewers for comments which helped us to improve this paper." to the Acknowledgements (L723-724)

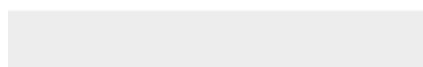
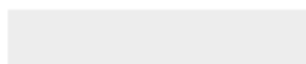
Thanks again for the helpful comments which have helped to improve this paper.



Click here to access/download

Additional Material for Reviewer Reference

wll_revised_jclimate_latexdiff.pdf



1 **Interactions between hydrological sensitivity, radiative cooling, stability and**
2 **low-level cloud amount feedback.**

3 MARK J. WEBB*

4 *Met Office Hadley Centre, UK*

5 ADRIAN P. LOCK

6 *Met Office, Exeter, UK.*

7 F. HUGO LAMBERT

8 *College of Engineering, Mathematics and Physical Sciences, University of Exeter, UK*

9 **Corresponding author address: Mark J. Webb, Met Office Hadley Centre, Exeter, EX1 3PB, UK.*

10 E-mail: mark.webb@metoffice.gov.uk

ABSTRACT

11 Low-level cloud feedbacks vary in magnitude, but are positive in most cli-
12 mate models, due to reductions in low-level cloud fraction. This study ex-
13 plores the impact of surface evaporation on low-level cloud fraction feedback
14 by performing climate change experiments with the aquaplanet configuration
15 of the HadGEM2-A climate model, forcing surface evaporation to increase at
16 different rates in two ways. Forcing the evaporation diagnosed in the surface
17 scheme to increase at 7%/K with warming (more than doubling the hydrolog-
18 ical sensitivity) results in an increase in global mean low-level cloud fraction
19 and a negative global cloud feedback, reversing the signs of these responses
20 compared to the standard experiments. The Estimated Inversion Strength
21 (EIS) increases more rapidly in these surface evaporation forced experiments,
22 which is attributed to additional latent heat release and enhanced warming
23 of the free troposphere. Stimulating a 7%/K increase in surface evaporation
24 via enhanced atmospheric radiative cooling however results in a weaker EIS
25 increase compared to the standard experiments and a slightly stronger low-
26 level cloud reduction. The low-level cloud fraction response is predicted bet-
27 ter by EIS than surface evaporation across all experiments. This suggests
28 that surface-forced increases in evaporation increase low-level cloud fraction
29 mainly by increasing EIS. Additionally our results show that increases in sur-
30 face evaporation can have a very substantial impact on the rate of increase
31 in radiative cooling with warming, by modifying the temperature and humid-
32 ity structure of the atmosphere. This has implications for understanding the
33 factors controlling hydrological sensitivity.

34 **1. Introduction**

35 Inter-model differences in cloud feedbacks constitute the largest source of spread in estimates
36 of equilibrium climate sensitivity in climate models, and this is primarily due to differences in the
37 responses of low clouds. While low-level cloud feedbacks vary substantially in magnitude, they
38 are positive in most models, where they are associated with reductions in low-level cloud fraction,
39 increasing the amount of solar radiation absorbed at the surface (Boucher et al. (2013)).

40 Many arguments have been advanced to explain the reduction in low-level cloudiness seen in
41 climate models with the warming climate. Rieck et al. (2012) proposed a mechanism where in-
42 creasing surface moisture fluxes would deepen the boundary layer, increase entrainment of dry
43 air from above the trade inversion, and reduce relative humidity and low-cloud fraction. Webb
44 and Lock (2013) argued that reductions in surface sensible heat and surface buoyancy fluxes with
45 warming could reduce turbulent moistening of the cloud layer. Brient and Bony (2013) proposed a
46 mechanism whereby increases in the vertical gradient of moist static energy in the warmer climate
47 result in a larger influx of low moist static energy and dry air into the boundary layer through
48 subsidence. Bretherton and Blossey (2014) proposed a mechanism related to that of Rieck et al.
49 (2012), whereby increases in cloud-layer humidity flux in the warmer climate lead to an entrain-
50 ment liquid-flux adjustment which dries the cloud layer. Sherwood et al. (2014) argued that verti-
51 cal mixing by large and small-scale processes would be expected to dry the boundary layer as the
52 climate warms. Following this, Brient et al. (2015) argued that low-cloud reductions in some mod-
53 els are caused by stronger convective mixing which dries the boundary layer more efficiently as
54 the surface warms, but that the low-cloud responses of many models are dominated by low-cloud
55 shallowing caused by weakened turbulent moistening.

56 It is recognised that the magnitude of any low-level cloud reduction will be determined by a num-
57 ber of competing factors (Rieck et al. (2012),Webb and Lock (2013),Zhang et al. (2013),Bretherton
58 et al. (2013),Blossey et al. (2013),Jones et al. (2014),Qu et al. (2015b),Vial et al. (2016)). While
59 factors which break up clouds may be dominant, their impact will be offset by other processes that,
60 if acting in isolation, would act to increase low-level cloud fraction. Such negative cloud feedback
61 mechanisms may include the effects of increasing stability on low cloud fraction (e.g. Blossey
62 et al. (2013),Qu et al. (2015b)) and enhanced moisture supply to the cloud layer from increasing
63 surface evaporation (e.g. Webb and Lock (2013),Zhang et al. (2013)). If we are to understand
64 why low-level cloud feedback is positive, it is therefore necessary to understand both positive and
65 negative low cloud feedback mechanisms and the reasons for their differing strengths.

66 One way to quantify the contribution of a hypothesized cloud feedback mechanism in a climate
67 model is to prevent it from operating in a climate change experiment, and to measure the impact
68 on the overall cloud feedback. Similarly a given mechanism may be strengthened to explore
69 the extent to which it compensates for other effects. Webb and Lock (2013) tested a number of
70 mechanisms in this way in the HadGEM2-A GCM, performing sensitivity experiments targeting
71 positive subtropical low cloud feedback. These included experiments where surface evaporation
72 was forced to increase at different rates, following similar sensitivity experiments with a very high
73 resolution process model run over a small domain representative of a trade cumulus boundary
74 layer (Rieck et al. (2012)).

75 The rate of increase in global mean surface evaporation and precipitation per degree warming
76 in a climate change scenario is often referred to as the hydrological sensitivity. As pointed out by
77 Fläschner et al. (2016), it is important to distinguish between estimates of hydrological sensitivity
78 which include temperature-independent effects of radiative forcing agents such as carbon dioxide
79 on the global precipitation increase and those which cleanly isolate the temperature-dependent

80 components. Here we use the term hydrological sensitivity to refer specifically to the temperature-
81 dependent increase in global precipitation with surface warming, excluding the effects of radiative
82 forcing agents, consistent with the approach of Mitchell et al. (1987), Lambert and Webb (2008),
83 Andrews et al. (2010) and Fläschner et al. (2016).

84 If relative humidity, surface wind speed and air sea temperature differences were to stay fixed
85 with future climate warming then global mean surface evaporation and precipitation would in-
86 crease at 7 %/K (Mitchell et al. (1987), Richter and Xie (2008), Rieck et al. (2012)). However,
87 the radiative cooling of the atmosphere is widely thought to regulate the hydrological sensitivity,
88 limiting the rate of increase of global mean surface evaporation and precipitation to something
89 closer to 3 %/K (e.g. Mitchell et al. (1987), Lambert and Webb (2008), Pendergrass and Hart-
90 mann (2014), Fläschner et al. (2016)). This is achieved through a combination of increases in
91 near-surface relative humidity and reductions in near-surface wind speed/air sea temperature dif-
92 ferences (e.g. Richter and Xie (2008)).

93 Webb and Lock (2013) noted that the surface evaporation in a region of strong subtropical cloud
94 feedback in the north-east Pacific between Hawaii and California increased very little in a climate
95 change experiments with HadGEM2-A, considerably less than the 3 %/K increase seen globally
96 and much less than the 7 %/K increase which would occur with warming in the absence of changes
97 in near-surface relative humidity, wind speed and air sea temperature difference. By forcing the lo-
98 cal surface evaporation to increase more strongly in the warmer climate, they were able to weaken
99 this local cloud feedback considerably, demonstrating that much of the positive low cloud feed-
100 back at that location could be attributed to the relatively weak increase in surface evaporation. A
101 limitation of that study was the fact that the surface evaporation was perturbed over a small region,
102 and one which focused on the location with the strongest low cloud feedback ; hence it was not
103 clear whether this mechanism explains the low cloud feedback more generally in this model.

104 More recently, highly idealised 'aqua planet' configurations of climate models forced with zon-
105 ally symmetric sea-surface temperatures (SSTs) have been shown to be remarkably successful in
106 reproducing the global cloud feedbacks predicted by climate models in realistic atmosphere only
107 and coupled ocean-atmosphere configurations (Ringer et al. (2014), Medeiros et al. (2015)).

108 In this study we apply the approach of Webb and Lock (2013) globally to investigate the positive
109 low-level cloud feedback in the aquaplanet configuration of HadGEM2-A. We pose the follow-
110 ing question: Does the muted (i.e. sub-7 %/K) increase in global surface evaporation contribute
111 substantially to the low cloud amount reduction and positive low cloud feedback? We test this
112 idea by performing climate change experiments with an SST forced 'aquaplanet' configuration of
113 HadGEM2-A which is subject to a uniform +4K SST perturbation, and where surface evapora-
114 tion is forced to increase at 7 %/K. We stimulate surface evaporation in two ways. In the first set
115 of experiments we add a term to the surface evaporation diagnosis which brings the zonal mean
116 evaporation in each time step into agreement with a target climatological value. In an additional
117 experiment we stimulate the hydrological cycle by adding an artificial radiative cooling term in
118 the atmosphere designed to approximately double the hydrological sensitivity.

119 Our model and experimental approach are described in more detail in Section 2. We present and
120 discuss our results in Section 3. We start by discussing the low cloud responses from the surface
121 evaporation forced experiments in Section 3a and those in the radiative cooling forced experiment
122 in Section 3b. We then go on to discuss the implications of our results for understanding the
123 hydrological sensitivity in Section 3c, and provide our concluding remarks in Section 4.

124 **2. Model Experiments and Methods**

125 We explore the impact of increasing surface evaporation on low-level cloud feedbacks in the
126 HadGEM2-A climate model (Martin et al. (2011)) by specifying surface evaporation following a

127 similar approach to that in Webb and Lock (2013), but at a global scale. Our experiments are sum-
128 marised in Table 1. The basis for our experiments is an aquaplanet configuration of HadGEM2-A
129 which is forced with time invariant, zonally and hemispherically symmetric sea surface tempera-
130 tures (SSTs), taken from the Aqua-Planet Experiment (APE) project 'Control' experiment (Neale
131 and Hoskins (2000)) (here denoted as APEC). This is accompanied by an idealised climate change
132 experiment, in which the APEC SSTs are subject to a uniform increase of 4K (APEC4K), follow-
133 ing the approach of Medeiros et al. (2015). The APEC and APEC4K experiments are referred to
134 throughout as the standard experiments. These differ slightly from the aqua planet experiments
135 in CMIP5, which were based on the APE 'Qobs' SSTs (Medeiros et al. (2015)). We chose the
136 APE 'Control' dataset, which has slightly more peaked SSTs in the tropics, as we found that, in
137 spite of their hemispherically symmetric forcings, the experiments based on the Qobs SSTs were
138 prone to having strong hemispherically asymmetric responses when we applied the surface evap-
139 oration forcing. We perform a number of sensitivity experiments based on the standard APEC
140 and APEC4K experiments in which we force the model to have various specified values of global
141 mean surface evaporation. We apply two approaches, which we call the surface evaporation forced
142 and radiative cooling forced methods.

143 For our first surface evaporation forced experiment (APECSurfaceEvap) we repeated APEC,
144 but forcing the zonal mean surface evaporation on each model time step to agree with the APEC
145 climatological zonal mean. This was done by diagnosing the surface evaporation in the usual
146 interactive manner and calculating the zonal mean at every model time step. A constant value
147 was then added at all points in a given line of latitude to force the zonal mean to agree with the
148 target value. This sets the zonal mean evaporation to the target value while retaining variations
149 along a line of latitude, maintaining synoptic structure in the surface evaporation field. Similarly
150 we repeated the APEC4K experiment, fixing the zonal mean surface evaporation to the zonal

151 mean climatology from APEC4K (APEC4KSurfaceEvap3%). These two experiments allow us
152 to assess whether or not the positive low cloud feedback can be reproduced with specified zonal
153 mean surface evaporation (see Section 3a). Two further experiments were then performed. In one
154 we repeated APEC4K, fixing the zonal mean surface evaporation to the climatology from APEC,
155 preventing the surface evaporation from increasing with warming (APEC4KSurfaceEvap0%). In
156 the other we forced the surface evaporation in the APEC4K experiment to increase at 7 %/K
157 relative to that in APEC specifying the zonal mean surface evaporation climatology from the APEC
158 experiment multiplied by a factor of 1.28 (APEC4KSurfaceEvap7%). This is what we would
159 expect to see for a warming without any changes in near-surface relative humidity, wind or air-sea
160 temperature difference.

161 For the radiative cooling forced experiments, we use the APEC experiment as the present day
162 control and force the global mean surface evaporation to increase more rapidly in an additional
163 +4K experiment (APEC4KRadCool7%) by artificially enhancing the atmospheric radiative cool-
164 ing rate. First we calculated the zonal mean climatology of the response in the clear-sky longwave
165 radiative heating rate between the APEC and APEC4K experiments as a function of height, which
166 takes negative values due to the radiative cooling increase. We then ran the APEC4KRadCool7%
167 experiment, adding this additional radiative cooling climatology (as a function of latitude and
168 height) to the actual radiative heating rate calculated by the model's radiation code in each model
169 timestep. This constitutes an extra $4.4 \text{ W/m}^2/\text{K}$ of atmospheric radiative cooling. We expected this
170 to approximately double the rate of increase in longwave clear-sky radiative cooling with warm-
171 ing, in turn approximately doubling the increase in global mean surface evaporation (see Section
172 3a).

173 All experiments were run for 72 months, and climatological means were formed over the full
174 period. As in many studies, we diagnose cloud feedbacks using the climatological mean change

175 in the cloud radiative effect (CRE) between the aquaplanet control and +4K experiments, divided
176 by the global mean near-surface temperature response. This can be considered a measure of cloud
177 feedback, including the climatological masking effects of clouds on the non-cloud feedbacks (see
178 Webb and Lock (2013) for a discussion of the merits of this approach compared to the alternatives).

179 **3. Results and Discussion**

180 *a. Low Cloud Responses in Surface Forced Evaporation Experiments*

181 Figure 1 shows the effects of forcing surface evaporation to increase at various different rates
182 with a uniform +4K warming applied to the HadGEM2-A aquaplanet configuration forced with
183 the APEC SSTs. Figure 1(a) shows the responses in zonal mean surface evaporation in the stan-
184 dard APEC4K experiment relative to APEC, and in the various experiments where surface evap-
185 oration is specified using the surface evaporation and radiative cooling forcing methods. The
186 global mean surface evaporation increases by $3.2 \text{ W/m}^2/\text{K}$ in the standard experiments APEC and
187 APEC4K, an increase of 3.4 \%/K relative to the global mean control value in APEC, which is 94.2
188 W/m^2 . As expected by design, the zonal mean evaporation increase in APEC4KSurfaceEvap3%
189 relative to APECSurfaceEvap (red line on Figure 1(a)) agrees well with that in the standard
190 experiments (black line), and APEC4KSurfaceEvap0% (orange line) shows no increase, while
191 APEC4KSurfaceEvap7% (blue line) shows an increase of 7.0 \%/K in the global mean, approxi-
192 mately twice that in the standard experiments. The APEC4KRadCool7% (green line) experiment
193 is also quite successful in reproducing an increase close to 7 \%/K , with a global mean increase
194 of 7.5 \%/K , with only minor differences in the meridional structure of the response. Figure 1(b)
195 shows the concomitant responses in zonal mean precipitation. We note some differences in the
196 precipitation responses in the APEC4K and APEC4KSurfEvap3% responses, with a tendency

197 for the precipitation to decrease at the equator and increase more on the flanks of the ITCZ in
198 APEC4KSurfEvap3% compared to the more concentrated increases seen in APEC4K. We do not
199 expect the responses in these experiments to be exactly the same, because the method used to force
200 the surface evaporation in the APEC4KSurfEvap3% experiment removes any temporal variability
201 in the zonal mean surface evaporation. The precipitation responses between the two experiments
202 are however much more consistent in the subtropical regions between 10-25° N/S where the posi-
203 tive low-level cloud feedbacks occur (see below).

204 Many previous studies have pointed out the association between positive subtropical cloud feed-
205 back and reductions in low-level cloud. The net cloud feedback (which we define here to include
206 cloud masking - see Section 2) in the standard experiments is positive in the global mean and
207 between 10 and 25° N/S, with the strongest positive feedback at 17° N/S (black line, Figure 1(c)).
208 The variations in the net cloud feedback are primarily due to the shortwave component (Figure
209 1(d)). Meanwhile the low cloud fraction reduces in the global mean and throughout the latitudes
210 where a positive net cloud feedback is present (black line, Figure 1(e)). The difference between
211 the surface-forced evaporation experiments APECSurfaceEvap and APEC4KSurfaceEvap3% suc-
212 cessfully reproduces the signs of the positive global mean cloud feedback and the global reduction
213 in low-level cloud fraction in the standard experiments, and also captures well the magnitudes of
214 their global responses. The zonal distributions of these quantities are also well captured (com-
215 pare black and red lines on Figure 1(c-e)). This demonstrates that the surface-forced evaporation
216 method does not substantially distort the cloud feedbacks, and is therefore a suitable method for
217 exploring the impact of differing levels of surface evaporation increase on cloud feedback.

218 Figures 1(c,e) also show that forcing the evaporation to increase at a rate closer to
219 7 %/K with a +4K warming using the surface evaporation forcing method (experiment
220 APEC4KSurfaceEvap7%, (blue line)) reverses the sign of both the global mean cloud feedback

221 and the low cloud fraction response, resulting in a negative global mean net cloud feedback and
222 an increase in global mean low cloud fraction. Although the signs of the global mean low-level
223 cloud fraction and cloud feedback responses reverse, the meridional structures of the responses
224 relative to their global means are not greatly affected. The most positive cloud feedback and the
225 associated low-level cloud fraction reduction located near to 15°N/S in the standard experiments
226 are not completely eradicated in the APEC4KSurfaceEvap7% experiment, indicating that part of
227 the positive cloud feedback in the APEC4K experiment cannot be explained by the muted increase
228 in surface evaporation.

229 One possible explanation for this might be that while increases in surface evaporation in the
230 climate change context generally increase low cloud fraction on occasions where there is little
231 mixing across the inversion, in a small fraction of cases where shallow convection is able to pene-
232 trate the inversion, enhanced surface evaporation might help to break up cloud. That said, the area
233 between the positive part of the curve and the zero line gives an indication of the contribution of
234 this remaining positive feedback to the global mean, which is small compared to the positive con-
235 tribution in the APEC/APEC4K experiments, and is dwarfed by that from the negative feedback
236 elsewhere.

237 The sensitivity of the global cloud feedback and low cloud response to the strength of the sur-
238 face evaporation increase is further demonstrated by the results from the APEC4KSurfaceEvap0%
239 experiment in which the surface evaporation does not increase at all with the warming climate; in
240 this scenario the global mean low cloud reduction is amplified compared to the standard experi-
241 ment and the global cloud feedback becomes more strongly positive (compare orange and black
242 lines on Figures 1(c,e)).

243 Our experiments also show substantial differences in the response of the Estimated Inversion
244 Strength (EIS, Wood and Bretherton (2006)) to climate warming (Figure 1(f)). EIS is a measure

245 of lower tropospheric stability which is based on the potential temperature difference between the
246 surface and 700 hPa level, and which gives an indication of the strength of low level temperature
247 inversions, for example those which are present at the top of subtropical boundary layers. EIS has
248 been shown to be a good predictor of spatio-temporal variations in low-level cloud fraction in the
249 present climate (Wood and Bretherton (2006)). Stronger values of EIS are generally associated
250 with a stronger capping inversions in subtropical boundary layers, which are widely thought to
251 encourage the formation and maintenance of low-level clouds by inhibiting entrainment of dry
252 air into the boundary layer from above and promoting shallow, well mixed boundary layers with
253 stratocumulus clouds which are strongly coupled to surface evaporation (Bretherton and Wyant
254 (1997), Wyant et al. (1997), Wood and Bretherton (2006)). Our results indicate that the magnitude
255 of the EIS response to the warming climate is very sensitive to the rate of the surface evaporation
256 increase in our surface-forced evaporation experiments, with a 7 %/K increase more than doubling
257 the magnitude of the EIS response compared to the standard case, and a modest EIS reduction in
258 the absence of an evaporation increase (Figure 1(f)). This suggests a second route whereby in-
259 creasing surface evaporation can increase low-level cloud fraction beyond the local argument put
260 forward in Webb and Lock (2013), namely that a stronger global increase in surface evaporation
261 results in stronger increases in EIS and stronger low level inversions in low cloud regimes, reduc-
262 ing drying of the boundary layer due to mixing with the free troposphere. Such an effect would
263 mean that the muted evaporation increase acts to reduce low-level cloud fraction more relative to
264 the 7 %/K scenario than would be expected via the local argument of Webb and Lock (2013) alone.

265 Why should the rate of increase in surface evaporation affect changes in EIS? Many studies
266 (e.g. Held and Soden (2006)) have suggested that the tropical lapse rate (the rate of decrease of
267 temperature with height) weakens in the warming climate because the free troposphere tends to
268 follow a temperature profile which is close to a moist adiabat, which becomes more statically sta-

269 ble with surface warming. A saturated adiabat has increasing potential temperature with height,
270 which strengthens as the lapse rate weakens with surface warming. Qu et al. (2015a) showed that
271 a number of climate models run in a similar aquaplanet configuration to that used here show in-
272 creases in potential temperature between 850 and 600 hPa which are too strong to be explained by
273 the moist adiabatic lapse rate argument alone. Figure 2(a) shows the increases in potential tem-
274 perature in our various experiments with warming in the tropical deep convection region centred
275 on the equator. In the surface-forced experiments, larger increases in surface evaporation are as-
276 sociated with larger levels of upper tropospheric warming and larger increases at 700 hPa relative
277 to the surface. In the APEC4KSurfaceEvap7% experiment in particular (blue line), the 700 hPa
278 potential temperature increases considerably more than would be predicted by the change in the
279 saturated moist adiabat. Figure 2(c) shows that in the APEC control experiment (gray line), the po-
280 tential temperature increases with altitude throughout the lower troposphere, at a rate which is less
281 than that predicted by a saturated adiabat. This is also the case for the APEC4KSurfaceEvap7%
282 experiment, although its profile is closer to a saturated adiabat than is the case in the APEC con-
283 trol experiment. Thus, while the increase in potential temperature with warming between APEC
284 and APEC4KSurfaceEvap7% at 700 hPa is more than that predicted by a change in the saturated
285 moist adiabat, the vertical potential temperature gradient does not exceed that predicted by the
286 moist adiabat in either of these experiments individually. This explains how the potential temper-
287 ature response at 700 hPa can be more than that predicted by a change in the saturated adiabat,
288 without violating the generally accepted principle that the absolute vertical potential temperature
289 gradient cannot exceed that predicted by a saturated adiabat. Similar behaviour is seen in the free
290 troposphere from 700 hPa upwards in the subtropics (Figures 2(b,d)).

291 Our interpretation of these results is as follows, and is summarised by the blue arrows in the
292 schematic in Figure 5. In the APEC4KSurfaceEvap7% experiment, the additional moisture sup-

293 ply into the boundary layer from the enhanced surface evaporation with climate warming will
294 increase near-surface humidity, generate convective instability and increase the amount of precipi-
295 tating deep convection, resulting in additional net latent heat release in regions of deep convection
296 (allowing for the effects of evaporating clouds and precipitation). This is supported by Figure 1(b)
297 which shows enhanced precipitation near the equator in APEC4KSurfaceEvap7% compared to
298 APEC4K. Figure 3 shows global mean heating and moistening rates from various components of
299 the model physics in our experiments. Our interpretation is also supported by Figure 3(a) which
300 shows enhanced heating by convection and cloud condensation above 700 hPa with increasing
301 surface-forced evaporation (see orange, red and blue lines). Enhanced free tropospheric warming
302 in convective regions of the tropics is then expected to propagate to the subtropics via horizontal
303 heat transport by tropical waves and the mean overturning circulation (Sobel et al. (2001)). This
304 will result in enhanced temperature increases in the free troposphere and reductions in the lapse
305 rate, increasing the amount by which the mid-upper free troposphere warms compared to the stan-
306 dard APEC4K experiment (compare blue and black lines on Figure 2(a,b)), and resulting in larger
307 increases in EIS (Figure 1(f)) and a stronger subtropical inversion. This would in turn result in
308 reduced entrainment of dry air into the boundary layer from above, and increasing (or weakening
309 reductions in) low-level cloud fraction. This interpretation could be tested further in the future
310 with additional sensitivity experiments - for example by artificially enhancing the rate of latent
311 heat release in the free troposphere with warming.

312 Figure 4 shows scatterplots of the responses in various global mean quantities. The differ-
313 ences in the global mean responses in the standard experiment (black symbols) compared to the
314 APEC4KSurfaceEvap0% experiment (orange symbols) are qualitatively similar to the differences
315 in the APEC4KSurfaceEvap7% experiment (blue symbols) compared to the standard experiments
316 (black symbols). Hence the arguments outlined above may be used to interpret both sets of re-

317 sponses to increasing surface evaporation. For example, in both cases stronger increases in surface
318 evaporation are associated with more positive EIS responses (Figure 4(a)), and weaker decreases
319 or stronger increases in low level cloud fraction (Figure 4(b)). The APEC4KSurfaceEvap0% ex-
320 periment does not show an increase in EIS, which indicates that we can attribute the increase
321 in EIS in the standard experiments to the increasing surface evaporation - i.e. the fact that the
322 hydrological sensitivity is positive.

323 It is interesting to note that modifying the surface-forced evaporation increase with warming in
324 both the APEC4KSurfaceEvap7% and APEC4KSurfaceEvap0% experiments affects the EIS and
325 low-cloud fraction responses and the net cloud feedback considerably poleward of 30° N/S (Figure
326 1). This suggests that the mechanisms discussed above are also relevant to understanding extra-
327 tropical cloud feedbacks. The standard experiments show a relatively weak net cloud feedback
328 here compared to the subtropics, in spite of substantial reductions in low cloud fraction (Figure
329 1). We attribute this partly to the fact that the annual mean insolation is less at higher latitudes,
330 and partly to compensating effects of changes in mid-high level clouds, condensed water path and
331 cloud phase changes. The surface-forced evaporation experiments clearly change the degree to
332 which these effects compensate for each other in contributing to the extra-tropical cloud feedback.
333 This may not only be because of the effects of changing stability on low cloud. Enhanced free-
334 tropospheric warming would also be expected to result in a stronger lifting of the freezing level.
335 This might strengthen negative phase change feedbacks associated with increasing mid-level cloud
336 fraction and albedo (e.g. Senior and Mitchell (1993)).

337 *b. Low Cloud Responses in Response to Enhanced Radiative Cooling.*

338 We now discuss the results from the experiment where we artificially increase the rate at
339 which the atmospheric radiative cooling increases with warming, thus stimulating the sur-

340 face evaporation indirectly. The global mean surface evaporation increases by a compara-
341 ble amount in APEC4KRadCool7% to that in the equivalent surface-forced evaporation ex-
342 periment APEC4KSurfaceEvap7% and the regional distribution of the surface evaporation in-
343 crease is also very similar (compare blue and green lines on Figure 1(a)). However the
344 cloud feedback and the cloud response is quite different; the net cloud feedback becomes
345 more positive in APEC4KRadCool7% rather than negative, and the low cloud fraction reduces
346 slightly more than in the standard experiments, rather than increasing strongly as it does in the
347 APEC4KSurfaceEvap7% experiment (Figure 1(c,e)). This very different cloud response with
348 warming given a similar surface evaporation increase indicates that the surface evaporation is
349 not the sole factor determining the different cloud feedbacks in our experiments. Figure 4(b)
350 shows a scatterplot of the global mean low cloud fraction response against the global surface
351 evaporation increase, and while this supports there being a relationship between surface evap-
352 oration and the low cloud fraction response in the surface-forced experiments, this relation-
353 ship is not maintained when the APEC4KRadCool7% experiment (green square) is included.
354 The EIS response in APEC4KRadCool7% (green) is also very different compared to that in
355 APEC4KSurfaceEvap7% (blue), being much weaker than that in the standard APEC4K experi-
356 ment (black), while APEC4KSurfaceEvap7% increases more strongly (Figure 4(a)).

357 Our interpretation of the different responses in APEC4KSurfaceEvap7% and
358 APEC4KRadCool7% is as follows, based loosely on the arguments of tropospheric energy
359 balance outlined by Mitchell et al. (1987). In the APEC4KSurfaceEvap7% experiment, as
360 argued above and as summarised by the blue lines in Figure 5, the additional moisture supply
361 at the surface will stimulate deep convection, resulting in additional latent heat release and free
362 tropospheric warming compared to that seen in the standard experiments, a reduced lapse rate, a
363 larger increase in EIS and an increase in low cloud fraction.

364 In the APEC4KRadCool7% experiment however (as indicated by the green arrows on Figure
365 5), the artificially enhanced radiative cooling (Figure 3(b)) will reduce the amount by which the
366 free troposphere warms compared to the standard APEC4K experiment (Figure 2(a,b)), resulting
367 in a more enhanced lapse rate and a reduced increase in EIS (Figure 1(f)). The enhanced lapse
368 rate will also make the atmosphere more convectively unstable and enhance precipitating deep
369 convection (Figure 1(b)). The additional latent heat release in the free troposphere (Figure 3(a))
370 will act to balance the imposed radiative cooling (Figure 3(b)). Near-surface relative humidity, air-
371 sea temperature differences and winds will adjust accordingly, increasing the surface evaporation
372 to balance the enhanced latent heat release. (This last aspect is explained in more detail in Section
373 3c below.)

374 The relatively small change in EIS in the APEC4KRadCool7% experiment compared to that in
375 the APEC4KSurfaceEvap7% experiment is consistent with the smaller low cloud response (Figure
376 1(a,b)), and Figure 4(c) shows that the global EIS response is in fact a better predictor of the low
377 cloud response across all of our experiments than is surface evaporation (cf Figure 4(b)). Figure
378 4(c) shows a linear regression line which fits the data very well, with a correlation coefficient of
379 0.98.

380 It is interesting to note that the relationship illustrated here shows a substantial reduction in low
381 cloud amount with warming in the absence of an EIS change, a reduction of 0.56 %/K as shown by
382 the intercept. The results from the APEC4KRadCool7% experiment reproduce this very well. The
383 slope of the regression line is 1.34 %/K. Wood and Bretherton (2006) found a regression slope of
384 6%/K for spatiotemporal variations in stratus cloud amount with EIS in observations. We would
385 not expect these numbers to agree however, for a number of reasons. One is that the global mean
386 low-cloud fractions used in our calculation are much smaller than those in the stratus cloud regions
387 examined by Wood and Bretherton (2006), in part because the global mean includes contributions

388 from areas with few low level clouds. Another is that the global mean low cloud fraction response
389 will include contributions from changes in other low cloud regimes (e.g. trade cumulus) whose
390 responses would not necessarily be expected to be the same as those in the stratus regions.

391 Although the main emphasis of this work is on understanding the role of changing surface evap-
392 oration on low cloud fraction feedback, it is interesting to note that it is in the absence of a surface
393 evaporation response that the strongest low cloud reduction is seen (Figure 4(b)). This suggests
394 that the underlying cause of the positive low cloud feedback in this model is not explained by
395 the surface evaporation and radiative cooling changes explored here (see the orange arrow on the
396 left hand side of the schematic in Figure 5). EIS reduces slightly in the APEC4KSurfaceEvap0%
397 experiment (Figure 4(c)) suggesting that the positive feedback is partly due to a reduction in EIS
398 in the absence of a surface evaporation increase. However substantial low cloud reductions are
399 also seen in the radiative cooling forced experiment in the absence of substantial changes in EIS,
400 indicating that other factors must also contribute to the positive low cloud feedbacks seen in the
401 absence of surface evaporation increases. For example, APEC4KSurfaceEvap0% shows a sub-
402 stantial drop in the in near-surface relative humidity (discussed below) which may be indicative of
403 a drop in relative humidity throughout the boundary layer, and which may in turn contribute to the
404 strong low cloud reduction.

405 In summary, we argue that increasing SSTs without allowing substantial changes in surface
406 evaporation or radiative cooling results in a reduction in low cloud fraction and a strong positive
407 cloud feedback (see orange arrows in Figure 5). Allowing surface evaporation to increase in re-
408 sponse to increasing SSTs stimulates convection and free tropospheric latent heat release, warming
409 the free troposphere, increasing EIS and opposing the reductions in low cloud fraction (blue arrows
410 on Figure 5). The net effect of these competing mechanisms in the standard experiment is a mod-
411 est reduction in low-level cloud fraction. (The thickness of the arrows in the schematic aim to give

412 an indication of the relative contribution of these two mechanisms in the standard experiment.)
413 Meanwhile, artificially enhancing the radiative cooling with climate warming reduces free tropo-
414 spheric warming, increases the lapse rate and weakens increases in EIS, slightly strengthening the
415 low cloud feedback compared to the standard experiment (green arrows on Figure 5).

416 It is interesting to contrast our findings with the widely accepted understanding of the mechanism
417 underlying the break up of clouds observed while following air masses undergoing the subtropical
418 stratocumulus to trade cumulus transition (Bretherton and Wyant (1997), Wyant et al. (1997), Qu
419 et al. (2015b)). Both scenarios relate to increasing surface temperatures and increasing surface
420 evaporation, but our argument suggests an increase in boundary layer cloud while the conven-
421 tional wisdom predicts the observed breakup of clouds. There are however important differences
422 between the two scenarios which can explain the differing responses. The observed Lagrangian
423 transition takes place in the context of a weakening trade inversion as SSTs increase while free
424 tropospheric temperatures change relatively little, producing conditions more favourable to mix-
425 ing or entrainment of dry air into the boundary layer from the free troposphere. In contrast, the
426 context of the climate change experiment is one where free tropospheric temperatures increase
427 faster than those at the surface, increasing the strength of the inversion and inhibiting cloud top
428 entrainment. As we have shown, this increasing inversion strength can in itself be a consequence
429 of a globally strengthening surface evaporation and hydrological cycle, which sets a very different
430 context to the situation in which we observe the Lagrangian stratocumulus to trade cumulus tran-
431 sition. Hence while the two scenarios may seem superficially similar from the point of view of the
432 surface evaporation increase, they are associated with opposite EIS changes. Therefore there is no
433 inconsistency between the interpretations of these two scenarios.

434 We have also considered the possibility that HadGEM2-A shows an increase in low-level cloud
435 in response to increasing surface-forced evaporation because it incorrectly captures the sign of

436 the low cloud fraction response under the subtropical stratocumulus to trade cumulus transition.
437 This is however not the case; HadGEM2-A does show a reduction in low-level cloud fraction
438 when forced with conditions representative of a subtropical marine low-level cloud transition from
439 stratocumulus to fair-weather cumulus (Neggers (2015)). HadGEM2-A also performs very well
440 in reproducing observed relationships between variability in low cloud fraction, SST and EIS (Qu
441 et al. (2015b)).

442 *c. Implications for understanding the hydrological sensitivity*

443 Our experiments also provide some new insights into the mechanisms which underlie the en-
444 hanced hydrological cycle in the warming climate. Many studies have pointed out that a change
445 in the global mean radiative cooling of the atmosphere will result in an equivalent response in
446 surface evaporation and precipitation, assuming that the sensible heat flux does not change sub-
447 stantially. For example, it has been shown that rapid precipitation adjustments in the absence of
448 surface temperature change which occur in response to various atmospheric radiative forcings can
449 be predicted accurately using offline radiation calculations which diagnose the effect of such ra-
450 diative forcings in the atmospheric radiative heating (e.g. Andrews et al. (2010)). In the case of
451 radiative forcings (e.g. due to carbon dioxide or black carbon) we do not expect that changes in
452 the hydrological cycle will affect the radiative forcings themselves. Hence we can say that in these
453 cases the perturbation in the radiative heating of the atmosphere is a good predictor of the hy-
454 drological cycle response. In the somewhat different case of climate warming however, previous
455 studies are unclear on the degree to which changes in surface latent heat fluxes affect atmospheric
456 radiative cooling. Here we show that increases in surface evaporation can have a very substantial
457 impact on the rate of increase in radiative cooling itself with warming. We use our experiments to
458 quantify the magnitude of this effect, and to explain how this dependence arises.

459 Figure 4(d) shows the changes in the main components of the global mean atmospheric energy
460 budget, which sum to zero. If increases in surface evaporation with warming did not influence
461 the radiative cooling, then we would expect to see the same radiative cooling response across the
462 surface-forced experiments, and the increase in surface evaporation would have to be balanced by
463 an equal and opposite decrease in the sensible heat flux. However, Figure 4(d) indicates that the
464 radiative cooling rate (indicated by the squares) increases by only a small amount ($0.6 \text{ W/m}^2/\text{K}$)
465 with warming when surface evaporation is held fixed in APEC4KSurfEvap0%, but increases pro-
466 gressively more with larger increases in surface evaporation in the surface-forced experiments by
467 ($2.6 \text{ W/m}^2/\text{K}$ in APEC4KSurfEvap3% and $4.9 \text{ W/m}^2/\text{K}$ in APEC4KSurfEvap7%). The general
468 agreement between the responses in the APEC4KSurfEvap3% experiment and standard APEC4K
469 experiment suggests that the radiative cooling increases in APEC4K are to a substantial degree a
470 consequence of the surface evaporation increases.

471 Our interpretation of this is as follows, and is summarised in Figure 5 (blue arrows). As shown
472 above, enhanced evaporation at the surface leads to enhanced free tropospheric warming (reduced
473 lapse rate). This would be expected to contribute to the larger increase in the atmospheric longwave
474 radiative cooling rate. This enhanced radiative cooling to space might be expected to be offset to
475 some extent by increases in specific humidity, assuming that upper-tropospheric relative humidity
476 does not change greatly (Ingram (2010)). However enhanced boundary layer specific humidity
477 may also enhance atmospheric radiative cooling by increasing the longwave radiation emitted
478 from the atmosphere to the surface (Pendergrass and Hartmann (2014)). (Note the increase in
479 near-surface specific humidity with increasing surface-forced evaporation shown in 4(e)). In the
480 absence of substantial changes in surface sensible heat flux, a new tropospheric energy balance
481 will be reached where the radiative cooling increases to a level which balances the enhanced net
482 latent heat release in the atmosphere, and equivalently the enhanced surface latent heat flux.

483 The regression line for the surface-forced experiments shown in Figure 4(d) indicates an in-
484 crease in radiative cooling of $0.6 \text{ W/m}^2/\text{K}$ with surface warming in the absence of an increase in
485 surface evaporation. The slope of the regression line indicates that the radiative cooling response
486 increases by $0.66 \text{ W/m}^2/\text{K}$ per unit increase in hydrological sensitivity in the surface-forced exper-
487 iments. Breaking this down into radiative heating components (not shown) indicates that the slope
488 is mainly attributable to the clear-sky longwave component ($-0.65 \text{ W/m}^2/\text{K}$), with $-0.1 \text{ W/m}^2/\text{K}$
489 coming from changes at the top-of-atmosphere and $-0.55 \text{ W/m}^2/\text{K}$ at the surface. This suggests
490 that the enhanced radiative cooling with increasing surface evaporation is primarily due to the im-
491 pact of changes in the temperature and humidity structure of the atmosphere on the downwelling
492 surface fluxes. This is consistent with the findings of Fläschner et al. (2016), who demonstrated
493 that the net effect of changes in humidity and lapse rate in the lower troposphere with warming is
494 to increase atmospheric radiative cooling.

495 Additionally the surface-forced evaporation experiments allow us to diagnose the dependence
496 of near-surface humidity, air-sea temperature difference and near-surface wind speed on changes
497 in surface evaporation, by cutting the feedback loop that normally operates to bring them into
498 balance as the climate warms. Similarly the APEC4KRadCool17% experiment allows us to see
499 how these quantities respond to changes in radiative cooling while maintaining these two-way
500 interactions near the surface. Together these experiments can inform our understanding of how
501 changes in these near-surface properties respond to and at the same time influence changes in
502 surface evaporation and radiative cooling.

503 The interactions discussed below are summarised in Figure 5. The colours give
504 an indication of the effects of increasing SST while holding surface evaporation fixed
505 (orange, as in APEC4KSurfaceEvap0%), increasing surface evaporation (blue, as in
506 APEC4KSurfaceEvap3% and APEC4KSurfaceEvap7%) and increasing radiative cooling (green,

507 as in APEC4KRadCool7%). Figure 4(f) shows that near-surface relative humidity drops with
508 climate warming when surface evaporation is held fixed, but increases with increasing surface-
509 forced evaporation. The near-surface relative humidity increases in the standard experiment, but
510 less so in the radiative cooling experiment. The differences in these responses cannot be explained
511 by changes in near-surface temperature; Figure 4(g) shows changes in air-minus-sea temperature
512 difference which, in the absence of changes in specific humidity, would be expected to have the
513 opposite effect on near-surface relative humidity. (Note that surface temperatures increase by 4K
514 everywhere in our experiments, so differences in air-sea temperature responses between our ex-
515 periments are solely due to differences in the near-surface temperature responses.) The reasons
516 for the air-sea temperature responses will be discussed below, but for now we can conclude that
517 the different responses in near-surface relative humidity are in the main due to differences in the
518 responses of the near-surface specific humidity (Figure 4(e)).

519 In general, near-surface specific humidity would be expected to be enhanced by increased sur-
520 face evaporation, but depleted by any enhanced vertical mixing by small-scale processes such
521 as convection, turbulence or resolved large-scale overturning (e.g. Sherwood et al. (2014)).
522 In the absence of increases in evaporation and assuming that other sink terms for near-surface
523 specific humidity do not change appreciably, we might expect only small changes in near-
524 surface specific humidity, and hence a drop in near-surface relative humidity with warming in
525 the APEC4KSurfaceEvap0% experiment. The near-surface specific humidity actually does in-
526 crease in the APEC4KSurfaceEvap0% experiment (Figure 4(e)), but less than half as much as in
527 the standard experiment, and not enough maintain the same near-surface relative humidity with
528 warming.

529 In the APEC4K, APEC4KSurfaceEvap3% and APEC4KSurfaceEvap7% experiments, progres-
530 sively larger increases in surface evaporation result in progressively stronger increases in near-

531 surface specific and relative humidity. Increasing surface-forced evaporation results in progres-
532 sively larger near-surface moistening rates from the boundary layer scheme, which distributes the
533 surface evaporation in the vertical via turbulent mixing (Figure 3(c)). The increasing near-surface
534 relative humidity in response to increasing surface evaporation will provide a negative feedback
535 on the surface evaporation and the hydrological sensitivity in the standard experiment.

536 Meanwhile, the APEC4KRadCool7% experiment shows slightly weaker increases in near-
537 surface humidity than in APEC4K in spite of a stronger increase in surface evaporation (Figure
538 4(e-f)) and the associated enhanced near-surface moistening rate from the boundary layer scheme
539 (Figure 3(c)). We attribute this to enhanced upward transport of near-surface humidity by convec-
540 tion in response to the enhanced radiative cooling. This is supported by Figure 3(d) which shows
541 enhanced convective drying of the boundary layer in APEC4KRadCool7% compared to APEC4K.
542 We argue that this enhanced convective drying reduces the near-surface humidity, resulting in an
543 increase in surface evaporation, and a new balance where the surface-evaporation-driven turbulent
544 moistening rate increases to balance the enhanced convective drying rate. The weaker increase in
545 near-surface humidity in the APEC4KRadCool7% experiment compared to the standard APEC4K
546 response is therefore part of the mechanism whereby the surface evaporation increases at a faster
547 rate in the APEC4KRadCool7% experiment.

548 In APEC4KSurfaceEvap0% the global mean near-surface temperature increases less than the
549 surface with warming, giving a small negative response in air-minus-sea temperature difference,
550 and an increase in the magnitude of the negative air-sea temperature difference (Figure 4(g)).
551 Our interpretation of this is as follows. Increasing the SST will initially increase the magnitude
552 of the air-sea temperature difference, resulting in a large increase in the sensible heat flux. The
553 near-surface air temperature will warm in response, providing a strong negative feedback on the
554 sensible heat flux increase until a balance is reached with a smaller increase than initially. This

555 is supported by Figure 4(d) which shows that the sensible heat flux does indeed increase slightly.
556 This will increase the surface buoyancy flux and enhance the vertical sensible heat transport by the
557 convection scheme. This is supported by the enhanced near-surface cooling seen in the convective
558 heating rates in Figure 3(a) in APEC4KSurfaceEvap0% (orange) compared to the APEC control
559 (grey) , and the increase in convective heating in the free troposphere. This in turn can explain
560 the enhanced warming in the upper troposphere in APEC4KSurfaceEvap0% (orange) compared
561 to APEC (grey) in Figure 2(c). The radiative cooling also increases slightly in the absence of an
562 increase in surface evaporation (Figure 4(d)), as would be expected given the increases in upper
563 tropospheric temperatures. Increases in near-surface specific humidity are also present (Figure
564 4(e)), but examination of the radiative cooling profile in Figure 3(b) indicates that the radiative
565 cooling is enhanced in the free troposphere rather than the boundary layer, suggesting that the
566 enhanced upper tropospheric temperatures are the main cause in this case. In the case of the
567 APEC4KSurfaceEvap0% experiment, tropospheric energy balance dictates that the changes in
568 radiative cooling and sensible heat flux must balance each other. The interpretation above explains
569 how the sensible heat flux and radiative cooling adjust to maintain tropospheric energy balance
570 with warming in the case where surface evaporation cannot change.

571 With the surface evaporation increases in the APEC4K, APECSurfaceEvap3% and APECSur-
572 faceEvap7% experiments, the sign of the response of the air-sea temperature difference reverses
573 compared to that in APEC4KSurfaceEvap0%, with the near-surface air temperature warming more
574 than the surface, and the magnitude of the (negative) air-sea temperature difference reducing (Fig-
575 ure 4(g)). Thus we can attribute the reduction in the magnitude of the air-sea temperature dif-
576 ference in the standard experiment to the effects of increasing surface evaporation. This is we
577 argue a result of enhanced latent heat release in the boundary layer, which is supported by Figure

578 3(a) which shows reduced cooling from the convection scheme from the surface up to 1km with
579 increasing surface evaporation.

580 The air-sea temperature difference changes little with warming in the APEC4KRadCool7% ex-
581 periment in contrast to the weakening in the magnitude of the air-sea temperature difference in
582 the standard experiments. We attribute this to an enhanced near-surface cooling rate from the
583 convection scheme in APEC4KRadCool7% compared to APEC4K (Figure 3(a)), due to enhanced
584 convection in response to the prescribed radiative cooling. The small change in the air-sea tem-
585 perature difference in APEC4KRadCool7% compared to the reduction in magnitude in APEC4K
586 will also contribute to the enhanced surface evaporation in APEC4KRadCool7%.

587 Additionally we note that responses in the sensible heat fluxes with warming (triangles on Fig-
588 ure 4(d)) are broadly consistent with what would be expected from the changes in the air-sea
589 temperature differences. The decreases of the sensible heat fluxes in response to increases in sur-
590 face evaporation and radiative cooling cannot be explained by the changes in the near-surface wind
591 speeds (Figure 4(h)), which increase in both cases. Hence these responses can largely be explained
592 in the same way as the air-sea temperature differences as outlined above. The increases in near-
593 surface winds will offset these effects to some degree, but not by enough to change the signs of
594 the responses. This means that the reduction in the global mean sensible heat flux with warming
595 in the standard experiment is a direct consequence of the increasing surface evaporation.

596 Near-surface wind speeds increase slightly on average with warming in the standard ex-
597 periments, more so in the APEC4KSurfaceEvap7% experiment, and even more so in the
598 APEC4KRadCool7% experiment, while they reduce in the APEC4KSurfaceEvap0% experiment
599 (Figure 4(h)). The change in the global mean surface wind speed is well correlated with the
600 change in the total radiative cooling (Figure 4(i)). Our interpretation of this is that the atmo-
601 spheric overturning circulation is enhanced by the progressively stronger radiatively-driven sub-

602 sidence in the subtropics. This effect will also contribute to the increased surface evaporation in
603 APEC4KRadCool7%.

604 To quantify the impact of these changes in near-surface properties on the interactively di-
605 agnosed surface evaporation, we decompose the hydrological sensitivities in APEC4K and
606 APEC4KRadCool7% into contributions from changes in SST, near-surface relative humidity, air-
607 minus-sea temperature difference and near-surface wind speed using the bulk formula for surface
608 evaporation (see Eq. 1 of Richter and Xie (2008)). We use linear regression to estimate a bulk tur-
609 bulent transfer coefficient suitable for use with local monthly mean values from the APEC experi-
610 ment, and then use the bulk formula to predict the surface evaporation responses in the APEC4K
611 and APEC4KRadCool7% experiments using local monthly mean values of SST and near-surface
612 properties. Long term averages of these predicted monthly values agree with the actual changes to
613 within 10-20%, while the difference in responses between APEC4KRadCool7% and APEC4K is
614 predicted to within 3% (Table 2). The changes in surface evaporation can be decomposed into con-
615 tributions from changes in SST and near-surface properties by repeating the calculations, adding
616 changes in each property to the calculation in turn. These calculations (Table 2) show that the
617 muted evaporation increase in the standard APEC4K experiment (weaker than the 7 %/K increase
618 which would occur with surface warming in the absence of changes in near-surface relative hu-
619 midity, wind speed and air sea temperature difference) is primarily due to increases in near-surface
620 relative humidity, but with a non-negligible contribution from increases in near-surface air tem-
621 perature which reduces the magnitude of the air-minus-sea temperature difference. The additional
622 surface evaporation in the APEC4KRadCool7% compared to APEC4K is primarily due to the en-
623 hanced near-surface winds, with a secondary contribution from the smaller increase in near-surface
624 relative humidity, and a more modest contribution from the smaller reduction in magnitude of the
625 air-sea temperature difference.

626 **4. Summary and Conclusions**

627 We explore the impact of surface evaporation and hydrological sensitivity on cloud feedback
628 by performing climate change experiments with the HadGEM2-A aquaplanet configuration where
629 surface evaporation is forced to increase at different rates, ranging from 0-7%/K. We modify the
630 surface evaporation response and global hydrological sensitivity firstly by specifying the evapo-
631 ration rate at the surface, and secondly by adding an artificial radiative cooling term in the atmo-
632 sphere.

633 Forcing the evaporation to increase at 7 %/K in the surface scheme in a uniform +4K SST per-
634 turbed experiment results in a negative global cloud feedback and an increase in global low cloud
635 fraction, reversing the signs of these responses compared to those in the standard model configura-
636 tion. Conversely the equivalent experiment with surface evaporation held fixed strongly increases
637 the magnitudes of the global mean low level cloud reduction and positive cloud feedback. In these
638 experiments, the estimated inversion strength (EIS, a measure of the lower tropospheric stability)
639 increases proportionally with the surface evaporation, due to enhanced free tropospheric warming
640 in response to additional latent heat release. We argue that this enhanced stabilisation of the tropics
641 results in a progressively more negative low cloud feedback with increasing surface-forced evapo-
642 ration, via the well established effect of lower tropospheric stability on low cloud fraction. Hence
643 our results demonstrate that modifying surface evaporation and global hydrological sensitivity can
644 have a substantial impact on the global low cloud feedback in a climate model, on a larger scale
645 than the local dependence on surface evaporation demonstrated by Webb and Lock (2013).

646 Additionally we force the surface evaporation to increase at 7 %/K by enhancing the rate at
647 which atmospheric radiative cooling increases with warming. In contrast to the surface-forced
648 evaporation increase, this reduces the free tropospheric warming, which weakens the increase in

649 EIS and slightly strengthens the low-level cloud reduction and the positive cloud feedback relative
650 to the standard experiments. Hence very different cloud feedbacks can arise in experiments with
651 similar hydrological sensitivities and changes in surface evaporation. This indicates that surface
652 evaporation is not the sole control on cloud feedback. Across all of the experiments performed, EIS
653 is a better predictor of low cloud feedback than surface evaporation. This suggests that surface-
654 forced increases in evaporation act to increase low cloud fraction mainly by increasing EIS. As
655 such our results also emphasise the important role that the free tropospheric temperature response
656 and the lower tropospheric stability play in low cloud feedback.

657 Although the main emphasis of this work is on understanding the role of changing surface evap-
658 oration on low cloud fraction feedback, it is interesting to note that it is in the absence of a surface
659 evaporation increase that the strongest low cloud reductions are seen. Substantial low cloud re-
660 ductions are also seen in the radiative cooling forced experiment , in the absence of substantial
661 changes in EIS. We do not explore the reasons for this further here, but note that experiments
662 where surface evaporation increases are prevented or where radiative cooling is perturbed may be
663 a useful vehicle for future investigation of the mechanisms responsible for breaking up low cloud
664 as the climate warms. Such experiments may help to separate positive cloud feedback mecha-
665 nisms from negative cloud feedback mechanisms associated with increases in surface evaporation
666 and EIS across cloud regimes, complementing existing approaches which have been used to sep-
667 arate competing terms statistically in specific cloud regimes (e.g. Qu et al. (2015b)). It should be
668 noted however that such experiments may not perfectly separate positive and negative feedbacks.

669 Inter-model differences in the strength of negative low cloud feedback mechanisms may also
670 contribute substantially to the overall spread in cloud feedback, in addition to the contribution
671 from positive mechanisms. As such, inter-model differences in hydrological sensitivity may also
672 contribute to inter-model spread in cloud feedback. Quantifying the extent to which positive low

673 cloud feedback mechanisms are offset by negative cloud feedback mechanisms such as those
674 demonstrated here may be a necessary step towards to understanding why low cloud feedbacks
675 are positive in models generally, and the extent to which this is true in nature.

676 Our experiments also provide new insights into the mechanisms underlying the hydrological
677 sensitivity. Many studies have pointed out that a change in the global mean radiative cooling of
678 the atmosphere will result in an equivalent response in surface evaporation and precipitation, as-
679 suming that the sensible heat flux does not change substantially, for example in the case of rapid
680 precipitation adjustments which occur following increases in carbon dioxide before substantial
681 surface warming occurs. In the somewhat different case of climate warming however, our re-
682 sults show that increases in surface evaporation can have a very substantial impact on the rate
683 of increase in radiative cooling. Increasing surface evaporation with surface warming modifies
684 the atmospheric temperature and humidity structure, substantially increasing the radiative cool-
685 ing. Conversely, holding surface evaporation fixed with warming yields only a small increase
686 in atmospheric radiative cooling. Hence, while models' different hydrological sensitivities can
687 usefully be interpreted using offline radiative decomposition methods (e.g. Pendergrass and Hart-
688 mann (2014)), DeAngelis et al. (2015), Fläschner et al. (2016)), it should be kept in mind that the
689 inputs to such radiative calculations (e.g. the profiles of the atmospheric temperature and humid-
690 ity changes) are themselves substantially affected by the rate of surface evaporation increase, and
691 hence the hydrological sensitivity.

692 We also show that near-surface relative humidity decreases with warming in the absence of in-
693 creasing surface evaporation, and hence that the increasing near-surface relative humidity in our
694 standard experiments is a direct consequence of increasing surface evaporation. This provides a
695 negative feedback on the surface evaporation and the hydrological sensitivity. Reductions in the
696 magnitude of the air-sea temperature difference and the surface sensible heat flux with warming

697 are also a consequence of the increasing surface evaporation; our results suggest that this is due
698 to enhanced near-surface warming associated with additional latent heat release in the boundary
699 layer. This effect also provides a negative feedback on the hydrological sensitivity. Meanwhile,
700 artificially enhancing the radiative cooling increase which accompanies surface warming reduces
701 the magnitude of near-surface increases in relative humidity by enhancing the rate at which con-
702 vection removes humidity from the boundary layer. Similarly enhanced removal of heat from the
703 boundary layer by convection increases the air-sea temperature difference. The additional radia-
704 tive cooling also increases near-surface wind speeds, presumably by enhancing radiatively-forced
705 subsidence. These effects explain how the surface evaporation increases to balance an externally
706 imposed radiative cooling of the atmosphere.

707 It is widely appreciated that increases in near-surface relative humidity will act to damp in-
708 creases in surface evaporation, while increases in the magnitude of air-sea temperature differences
709 and near-surface wind speeds will act to enhance it. Our results also demonstrate however that the
710 responses in the factors controlling the surface evaporation (such as near-surface relative humidity,
711 wind speed and air-sea temperature differences) are affected not only by radiative cooling but also
712 by changes in surface evaporation itself. We argue that the hydrological sensitivity will ultimately
713 be determined by the point at which various interacting responses in near-surface relative humid-
714 ity and wind speed, air-sea temperature difference, surface evaporation, sensible heat fluxes and
715 radiative cooling come into a new balance following a given surface warming. This means that
716 a full understanding of the mechanisms controlling hydrological sensitivity differences in models
717 will require a better appreciation of these various inter-dependent responses. These insights may
718 help to improve our understanding of the factors controlling hydrological sensitivity in the future.

719 *Acknowledgments.* We are grateful to Tim Andrews, Chris Bretherton, Paulo Ceppi, William In-
720 gram, Jonathan Gregory, Steve Klein, Angeline Pendergrass, Mark Ringer, Jack Scheff, Graeme
721 Stephens and Alison Stirling for useful discussions about this work. We would also like to ac-
722 knowledge Yoko Tsushima and Rachel Stratton for help in calculating APE APEC SST forcings,
723 and Alison Stirling for providing code to calculate saturated adiabats. We are also grateful to Karen
724 Shell and two anonymous reviewers for comments which helped us to improve this paper. Mark
725 Webb was supported by the Joint UK BEIS/Defra Met Office Hadley Centre Climate Programme
726 (GA01101).

727 **References**

- 728 Andrews, T., P. M. Forster, O. Boucher, N. Bellouin, and A. Jones, 2010: Precipitation, radiative
729 forcing and global temperature change. *Geophysical Research Letters*, **37** (14).
- 730 Blossey, P. N., and Coauthors, 2013: Marine low cloud sensitivity to an idealized climate change:
731 The CGILS LES intercomparison. *Journal of Advances in Modeling Earth Systems*, **5** (2), 234–
732 258.
- 733 Boucher, O., and Coauthors, 2013: Clouds and aerosols. *Climate Change 2013: The physical*
734 *science basis. Contribution of working group I to the Fifth Assessment Report of the Intergov-*
735 *ernmental Panel on Climate Change*, Cambridge University Press, 571–657.
- 736 Bretherton, C. S., and P. N. Blossey, 2014: Low cloud reduction in a greenhouse-warmed climate:
737 Results from Lagrangian LES of a subtropical marine cloudiness transition. *Journal of Advances*
738 *in Modeling Earth Systems*, **6** (1), 91–114.
- 739 Bretherton, C. S., P. N. Blossey, and C. R. Jones, 2013: Mechanisms of marine low cloud sensi-
740 tivity to idealized climate perturbations: A single-LES exploration extending the CGILS cases.

741 *Journal of Advances in Modeling Earth Systems*, **5** (2), 316–337.

742 Bretherton, C. S., and M. C. Wyant, 1997: Moisture transport, lower-tropospheric stability, and
743 decoupling of cloud-topped boundary layers. *Journal of the atmospheric sciences*, **54** (1), 148–
744 167.

745 Brient, F., and S. Bony, 2013: Interpretation of the positive low-cloud feedback predicted by a
746 climate model under global warming. *Climate Dynamics*, **40** (9-10), 2415–2431.

747 Brient, F., T. Schneider, Z. Tan, S. Bony, X. Qu, and A. Hall, 2015: Shallowness of tropical low
748 clouds as a predictor of climate models’ response to warming. *Climate Dynamics*, 1–17.

749 DeAngelis, A. M., X. Qu, M. D. Zelinka, and A. Hall, 2015: An observational radiative constraint
750 on hydrologic cycle intensification. *Nature*, **528** (7581), 249–253.

751 Fläschner, D., T. Mauritsen, and B. Stevens, 2016: Understanding the intermodel spread in global-
752 mean hydrological sensitivity. *Journal of Climate*, **29** (2), 801–817.

753 Held, I. M., and B. J. Soden, 2006: Robust responses of the hydrological cycle to global warming.
754 *Journal of Climate*, **19** (21), 5686–5699.

755 Ingram, W., 2010: A very simple model for the water vapour feedback on climate change. *Quar-*
756 *terly Journal of the Royal Meteorological Society*, **136** (646), 30–40.

757 Jones, C., C. Bretherton, and P. Blossey, 2014: Fast stratocumulus time scale in mixed layer model
758 and large eddy simulation. *Journal of Advances in Modeling Earth Systems*, **6** (1), 206–222.

759 Lambert, F. H., and M. J. Webb, 2008: Dependency of global mean precipitation on surface tem-
760 perature. *Geophysical Research Letters*, **35** (16).

761 Martin, G., and Coauthors, 2011: The HadGEM2 family of met office unified model climate
762 configurations. *Geoscientific Model Development Discussions*, **4**, 765–841.

763 Medeiros, B., B. Stevens, and S. Bony, 2015: Using aquaplanets to understand the robust responses
764 of comprehensive climate models to forcing. *Climate Dynamics*, **44 (7-8)**, 1957–1977.

765 Mitchell, J. F., C. Wilson, and W. Cunnington, 1987: On CO₂ climate sensitivity and model
766 dependence of results. *Quarterly Journal of the Royal Meteorological Society*, **113 (475)**, 293–
767 322.

768 Neale, R. B., and B. J. Hoskins, 2000: A standard test for AGCMs including their physical
769 parametrizations: I: The proposal. *Atmospheric Science Letters*, **1 (2)**, 101–107.

770 Neggers, R., 2015: Attributing the behavior of low-level clouds in large-scale models to subgrid-
771 scale parameterizations. *Journal of Advances in Modeling Earth Systems*, **7 (4)**, 2029–2043.

772 Pendergrass, A. G., and D. L. Hartmann, 2014: The atmospheric energy constraint on global-mean
773 precipitation change. *Journal of Climate*, **27 (2)**, 757–768.

774 Qu, X., A. Hall, S. A. Klein, and P. M. Caldwell, 2015a: The strength of the tropical inversion and
775 its response to climate change in 18 CMIP5 models. *Climate Dynamics*, **45 (1-2)**, 375–396.

776 Qu, X., A. Hall, S. A. Klein, and A. M. DeAngelis, 2015b: Positive tropical marine low-cloud
777 cover feedback inferred from cloud-controlling factors. *Geophysical Research Letters*, **42 (18)**,
778 7767–7775.

779 Richter, I., and S.-P. Xie, 2008: Muted precipitation increase in global warming simulations: A
780 surface evaporation perspective. *Journal of Geophysical Research: Atmospheres*, **113 (D24)**.

781 Rieck, M., L. Nuijens, and B. Stevens, 2012: Marine boundary layer cloud feedbacks in a constant
782 relative humidity atmosphere. *Journal of the Atmospheric Sciences*, **69 (8)**, 2538–2550.

783 Ringer, M. A., T. Andrews, and M. J. Webb, 2014: Global-mean radiative feedbacks and forcing
784 in atmosphere-only and coupled atmosphere-ocean climate change experiments. *Geophysical*
785 *Research Letters*, **41** (11), 4035–4042.

786 Senior, C., and J. Mitchell, 1993: Carbon dioxide and climate. the impact of cloud parameteriza-
787 tion. *Journal of Climate*, **6** (3), 393–418.

788 Sherwood, S. C., S. Bony, and J.-L. Dufresne, 2014: Spread in model climate sensitivity traced to
789 atmospheric convective mixing. *Nature*, **505** (7481), 37–42.

790 Sobel, A. H., J. Nilsson, and L. M. Polvani, 2001: The weak temperature gradient approximation
791 and balanced tropical moisture waves. *Journal of the Atmospheric Sciences*, **58** (23), 3650–
792 3665.

793 Vial, J., S. Bony, J.-L. Dufresne, and R. Roehrig, 2016: Coupling between lower-tropospheric
794 convective mixing and low-level clouds: Physical mechanisms and dependence on convection
795 scheme. *Journal of Advances in Modeling Earth Systems*, doi:10.1002/2016MS000740, URL
796 <http://dx.doi.org/10.1002/2016MS000740>.

797 Webb, M. J., and A. P. Lock, 2013: Coupling between subtropical cloud feedback and the local
798 hydrological cycle in a climate model. *Climate dynamics*, **41** (7-8), 1923–1939.

799 Wood, R., and C. S. Bretherton, 2006: On the relationship between stratiform low cloud cover and
800 lower-tropospheric stability. *Journal of Climate*, **19** (24), 6425–6432.

801 Wyant, M. C., C. S. Bretherton, H. A. Rand, and D. E. Stevens, 1997: Numerical simulations and
802 a conceptual model of the stratocumulus to trade cumulus transition. *Journal of the atmospheric*
803 *sciences*, **54** (1), 168–192.

804 Zhang, M., and Coauthors, 2013: CGILS: Results from the first phase of an international project to
805 understand the physical mechanisms of low cloud feedbacks in single column models. *Journal*
806 *of Advances in Modeling Earth Systems*, **5** (4), 826–842.

807 **LIST OF TABLES**

808 **Table 1.** Experiment names and descriptions. 38

809 **Table 2.** Decomposition of surface evaporation responses in APEC4K and
810 APEC4KRadCool7% experiments. 39

TABLE 1. Experiment names and descriptions.

Experiment	Description
APEC	Aquaplanet experiment based on APE Control SSTs
APEC4K	As APEC with a uniform +4K SST perturbation
APECSurfaceEvap	APEC SST/surface evaporation forced to APEC zonal climatology
APEC4KSurfaceEvap0%	APEC4K SST/surface-forced evaporation to APEC zonal climatology
APEC4KSurfaceEvap3%	APEC4K SST/surface-forced evaporation to APEC4K zonal climatology
APEC4KSurfaceEvap7%	APEC4K SST/surface-forced evaporation 7%/K increase from APEC
APEC4KRadCool7%	APEC4K SST with enhanced atmospheric radiative cooling

TABLE 2. Decomposition of surface evaporation responses in APEC4K and APEC4KRadCool7% experiments.

W/m²/K	APEC4K	APEC4KRadCool7%	APEC4KRadCool7% - APEC4K
Surface Evaporation Response	3.2	7.1	3.9
Predicted Surface Evaporation Response	3.8	7.8	4.0
SST Component	6.8	6.8	0.0
Near-Surface Relative Humidity Component	-2.0	-0.6	1.4
Air-Sea Temperature Difference Component	-0.8	-0.1	0.7
Near-Surface Wind Speed Component	-0.1	1.8	1.9

811

LIST OF FIGURES

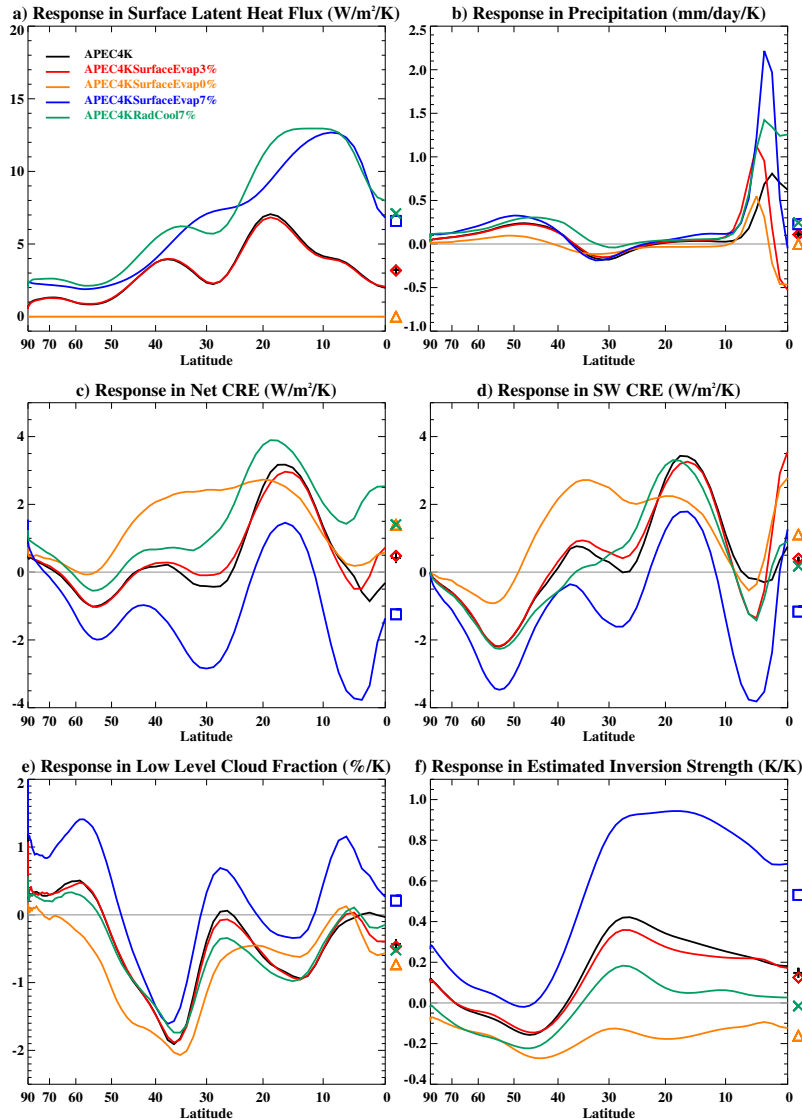
812 **Fig. 1.** Responses to a uniform +4K SST increase in aquaplanet experiments forced with APE Control (APEC) SSTs and varying degrees of surface evaporation increase (see Table 1). a) Surface latent heat flux, b) precipitation, c) net (longwave plus shortwave) Cloud Radiative Effect (CRE), d) shortwave CRE, e) maximum low-level cloud fraction and f) Estimated Inversion Strength (EIS). Both hemispheres are averaged and results are plotted as a non-uniform function of latitude such that the area under the curve gives a good indication of the contribution to the global mean from different latitudes. The APEC4K and APEC4KRadCool7% responses are relative to APEC while the surface-forced experiment responses are relative to APECSurfaceEvap. All are divided by 4 so as to be expressed per K warming. The global mean responses are indicated by symbols on the right hand side. 41

822 **Fig. 2.** Responses in profiles of potential temperature to uniform +4K warming averaged over the areas between a) 10°N - 10°S and b) 10-30°N/S from the same experiments as shown in Figure 1. The response in the saturated moist adiabat associated with surface temperature increases ranging from 2 to 8K in 1K increments over the region 10°N - 10°S are shown as dashed lines on a) and b). c) and d) show absolute profiles of potential temperature in the various experiments averaged 10°N - 10°S and 10-30°N/S respectively. The gray lines show the APEC control experiment and the coloured lines show the various +4K experiments. Saturated adiabats are plotted as dashed lines for the control SSTs over the region 10°N - 10° and for surface temperatures 5 and 10K warmer. The horizontal lines show the heights of the 700 and 200 hPa levels. 42

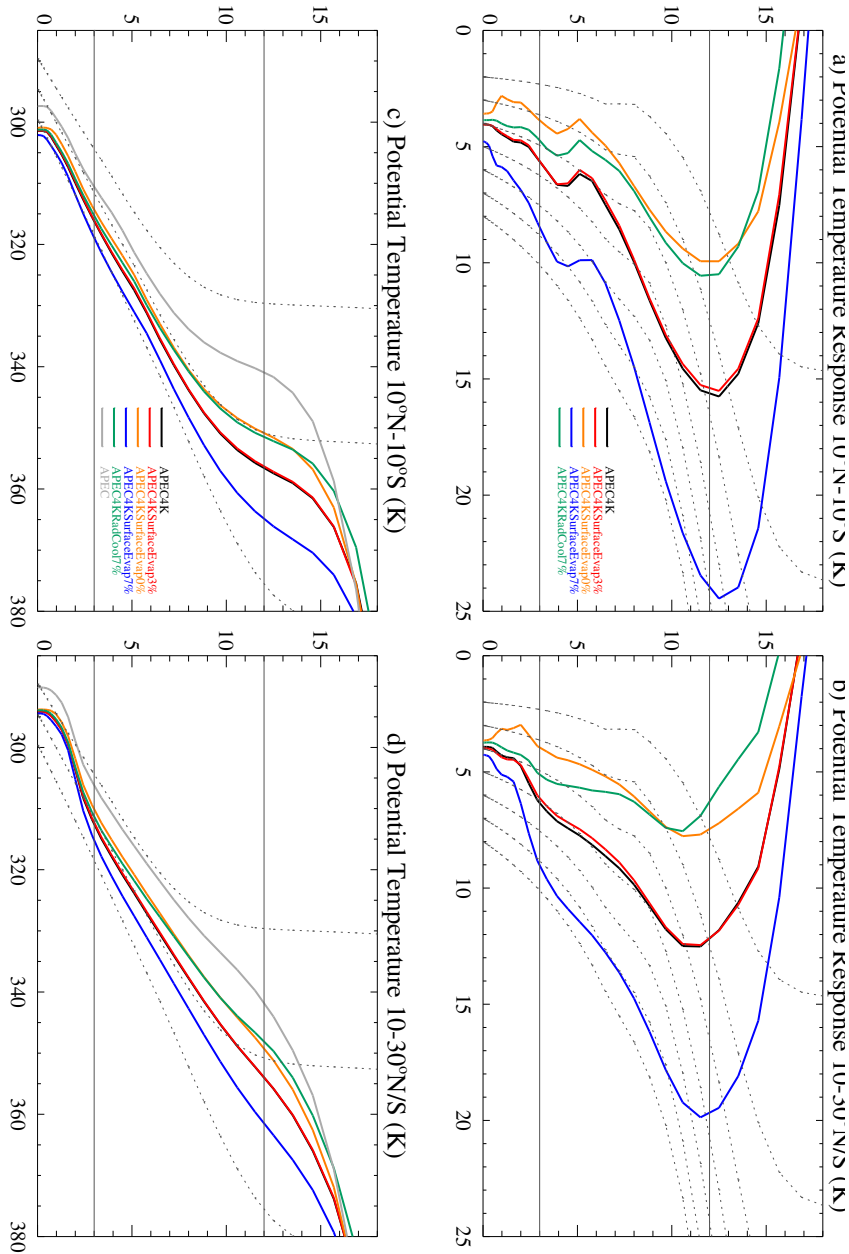
832 **Fig. 3.** Global mean atmospheric heating and moistening rates from radiation, boundary layer, convection and cloud schemes. a) heating rates from convection b) heating rates from radiation c) net moistening rates from surface evaporation, boundary layer and large scale cloud condensation d) moistening rates from convection. The lines below the x axis indicate the values in the bottom model level, with the APEC experiment denoted by a vertical gray line and the various +4K experiments denoted by + symbols. The horizontal line shows the height of the 700 hPa level. 43

839 **Fig. 4.** Scatterplots of global mean responses, expressed per K surface warming. a) Estimated Inversion Strength (EIS) against surface evaporation. b) low cloud fraction against surface evaporation. c) low cloud fraction against EIS. d) responses in surface evaporation (plus signs), atmospheric radiative heating rate (squares) and surface sensible heat flux (triangles) against surface evaporation. e)-h) near-surface specific and relative humidity, air-minus-surface temperature difference and 10m near-surface wind speed against surface evaporation. i) 10m near-surface wind speed against atmospheric radiative heating. The grey lines on c) and i) show fits to all five data points. The grey line on d) is a fit to the radiative heating responses for the surface-forced experiments only. 44

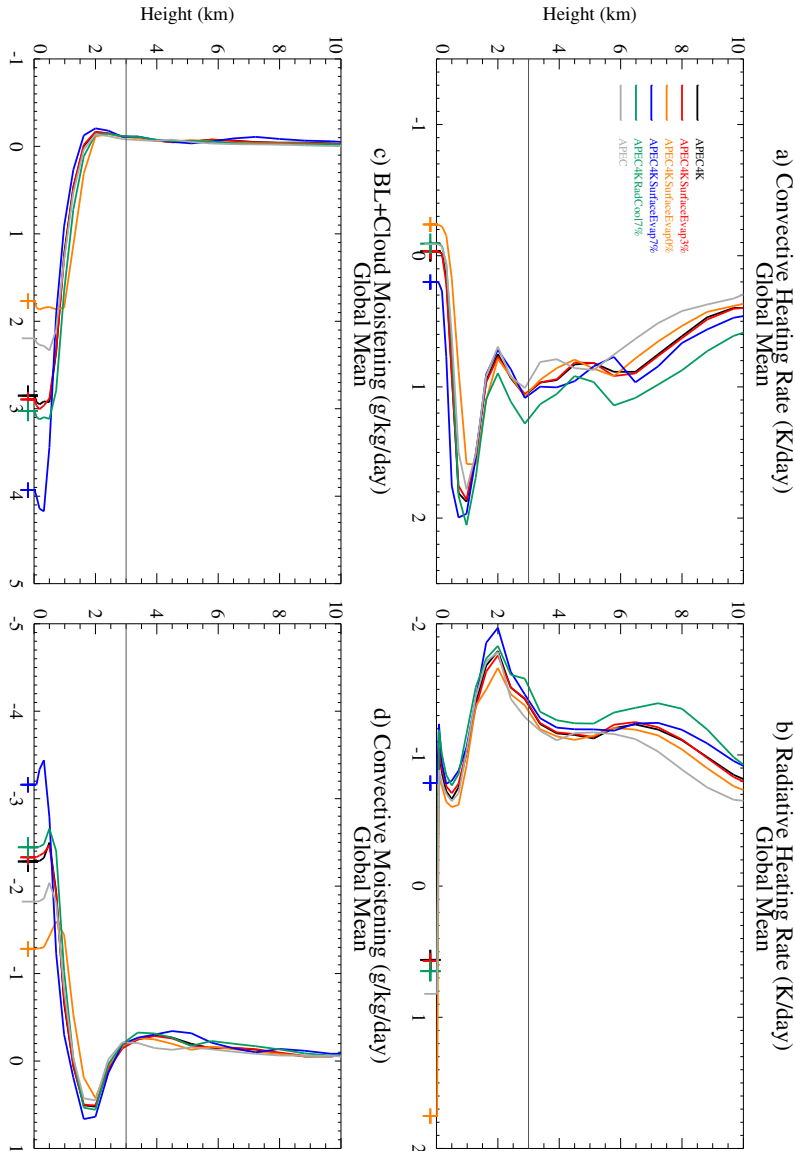
848 **Fig. 5.** Schematic summarising interactions between global mean surface evaporation, radiative cooling, stability and low-level cloud fraction. All quantities are positive, with plus and minus signs indicating increasing and decreasing magnitude respectively. The colours give an indication of the effects of increasing SST while holding surface evaporation fixed (orange), increasing surface evaporation (blue) and increasing radiative cooling (green). The black plus signs inside the boxes show the sign of the changes in the standard APEC4K experiment, and the thicknesses of the lines have been chosen to give an indication of the importance of the various interactions for determining the responses in APEC4K. 45



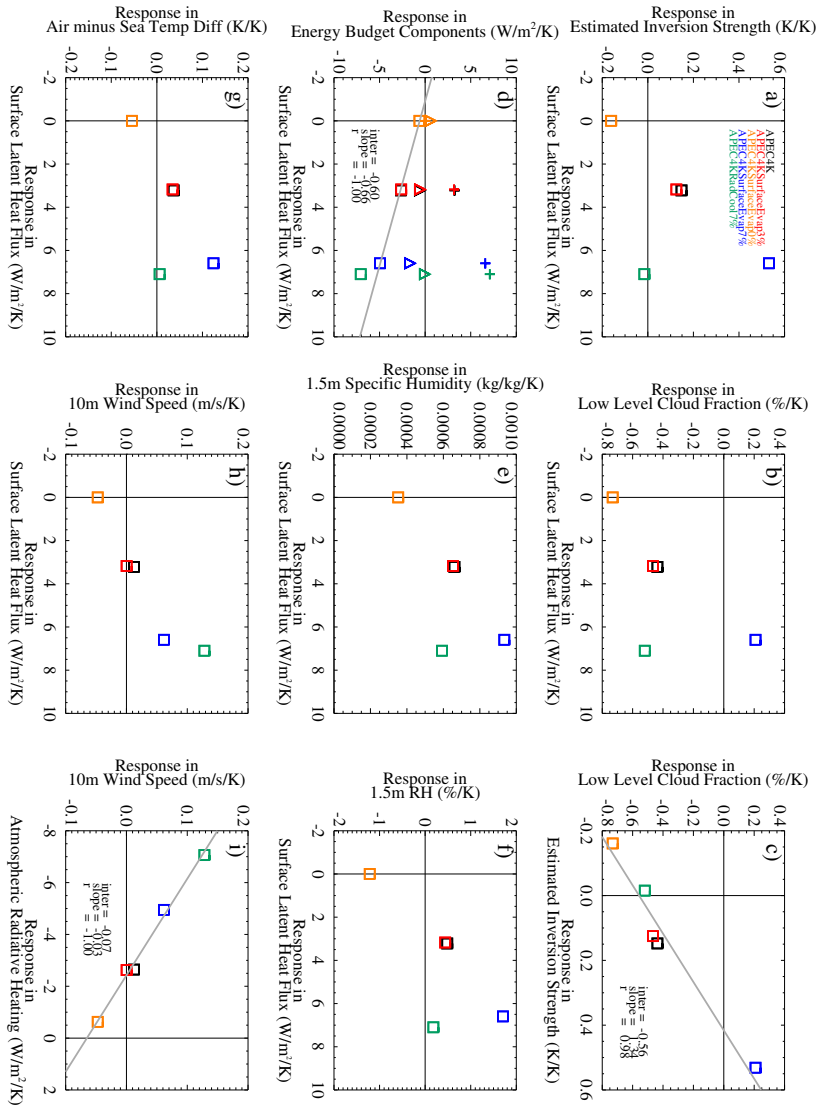
856 FIG. 1. Responses to a uniform +4K SST increase in aquaplanet experiments forced with APE Control
 857 (APEC) SSTs and varying degrees of surface evaporation increase (see Table 1). a) Surface latent heat flux, b)
 858 precipitation, c) net (longwave plus shortwave) Cloud Radiative Effect (CRE), d) shortwave CRE, e) maximum
 859 low-level cloud fraction and f) Estimated Inversion Strength (EIS). Both hemispheres are averaged and results
 860 are plotted as a non-uniform function of latitude such that the area under the curve gives a good indication of
 861 the contribution to the global mean from different latitudes. The APEC4K and APEC4KRadCool7% responses
 862 are relative to APEC while the surface-forced experiment responses are relative to APECSurfaceEvap. All are
 863 divided by 4 so as to be expressed per K warming. The global mean responses are indicated by symbols on the
 864 right hand side.



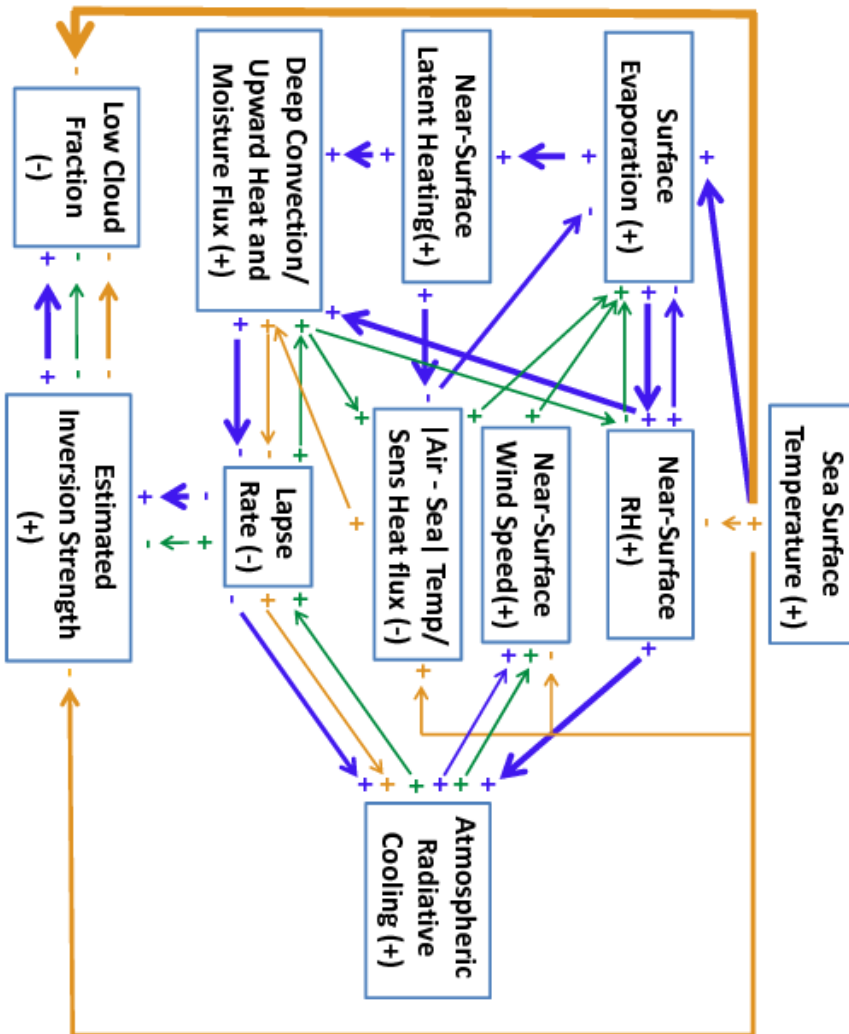
865 FIG. 2. Responses in profiles of potential temperature to uniform +4K warming averaged over the areas
 866 between a) 10°N - 10°S and b) 10-30°N/S from the same experiments as shown in Figure 1. The response in the
 867 saturated moist adiabat associated with surface temperature increases ranging from 2 to 8K in 1K increments
 868 over the region 10°N - 10°S are shown as dashed lines on a) and b). c) and d) show absolute profiles of potential
 869 temperature in the various experiments averaged 10°N - 10°S and 10-30°N/S respectively. The gray lines show
 870 the APEC control experiment and the coloured lines show the various +4K experiments. Saturated adiabats are
 871 plotted as dashed lines for the control SSTs over the region 10°N - 10° and for surface temperatures 5 and 10K
 872 warmer. The horizontal lines show the heights of the 700 and 200 hPa levels.



873 FIG. 3. Global mean atmospheric heating and moistening rates from radiation, boundary layer, convection
 874 and cloud schemes. a) heating rates from convection b) heating rates from radiation c) net moistening rates from
 875 surface evaporation, boundary layer and large scale cloud condensation d) moistening rates from convection.
 876 The lines below the x axis indicate the values in the bottom model level, with the APEC experiment denoted
 877 by a vertical gray line and the various +4K experiments denoted by + symbols. The horizontal line shows the
 878 height of the 700 hPa level.



879 FIG. 4. Scatterplots of global mean responses, expressed per K surface warming. a) Estimated Inversion
 880 Strength (EIS) against surface evaporation. b) low cloud fraction against surface evaporation. c) low cloud frac-
 881 tion against EIS. d) responses in surface evaporation (plus signs), atmospheric radiative heating rate (squares)
 882 and surface sensible heat flux (triangles) against surface evaporation. e-h) near-surface specific and relative hu-
 883 midity, air-minus-surface temperature difference and 10m near-surface wind speed against surface evaporation.
 884 i) 10m near-surface wind speed against atmospheric radiative heating. The grey lines on c) and i) show fits to all
 885 five data points. The grey line on d) is a fit to the radiative heating responses for the surface-forced experiments
 886 only.



887 FIG. 5. Schematic summarising interactions between global mean surface evaporation, radiative cooling,
 888 stability and low-level cloud fraction. All quantities are positive, with plus and minus signs indicat-
 889 ing and decreasing magnitude respectively. The colours give an indication of the effects of increasing SST
 890 while holding surface evaporation fixed (orange), increasing surface evaporation (blue) and increasing radiative
 891 cooling (green). The black plus signs inside the boxes show the sign of the changes in the standard APEC4K
 892 experiment, and the thicknesses of the lines have been chosen to give an indication of the importance of the
 893 various interactions for determining the responses in APEC4K.